

## Spatio-Temporal Graph Neural Network for Solar Irradiance Prediction: A Case Study in Nganjuk, Indonesia

Agung Wilis Nurcahyo<sup>1</sup>, Bambang Purnomosidi Dwi Putranto<sup>2</sup>

<sup>1</sup>Master of Information Technology, Universitas Teknologi Digital Indonesia, Yogyakarta, Indonesia

<sup>2</sup>Department of Information Technology, Universitas Teknologi Digital Indonesia, Yogyakarta, Indonesia

<sup>1</sup>Meteorological, Climatological, and Geophysical Agency (BMKG), Nganjuk, Indonesia

### Received:

November 28, 2025

### Revised:

January 15, 2026

### Accepted:

January 28, 2026

### Published:

February 25, 2026

Corresponding Author:

### Author Name\*:

Bambang Purnomosidi Dwi Putranto

### Email\*:

bdpdp@utdi.ac.id

DOI:

10.63158/journalisi.v8i1.1424

© 2026 Journal of Information Systems and Informatics. This open access article is distributed under a (CC-BY License)



**Abstract.** Solar energy utilization in tropical regions is strongly influenced by the accuracy of solar irradiance estimation, which is affected by temporal variability and spatial atmospheric interactions. Conventional forecasting approaches commonly rely on single-station time-series models, limiting their ability to capture regional dependencies. This study proposes a spatio-temporal modeling framework based on Graph Neural Networks (GNN) to estimate solar irradiance by explicitly incorporating spatial relationships among observation sites. The study focuses on Sawahan Subdistrict, Nganjuk Regency, Indonesia, using solar irradiance data collected from five Automatic Weather Stations (AWS) operated by the Indonesian Agency for Meteorology, Climatology, and Geophysics (BMKG) during 2024. Each station is represented as a graph node, with spatial connections constructed based on geographical distance, while temporal dependencies are modeled using Long Short-Term Memory (LSTM). Experimental results show that the proposed model achieves a Mean Absolute Error (MAE) of 102.64 W/m<sup>2</sup>, a Root Mean Squared Error (RMSE) of 166.76 W/m<sup>2</sup>, and an R<sup>2</sup> value of 0.6446 for the target location. These findings demonstrate that GNN-based spatial aggregation improves estimation stability and accuracy, providing practical support for localized solar energy assessment in tropical regions.

**Keywords:** Graph Neural Network; Solar Irradiance Estimation; Spatio-Temporal Modeling; Automatic Weather Station; Renewable Energy Forecasting

## 1. INTRODUCTION

The continuously increasing global energy demand is accelerating the transition towards sustainable renewable energy sources, one of which is solar energy [1], [2]. As a tropical country, Indonesia has high solar radiation potential throughout the year, making it highly prospective for region-based solar energy development [3]. However, the utilization of this potential still faces a major challenge in the form of uncertainty and variability in solar radiation due to temporal and spatial atmospheric dynamics [4].

Most early research on solar radiation estimation relied on statistical approaches and conventional time-series models, such as linear regression and ARIMA [5], [6], [7]. Although these methods are relatively simple and easy to implement, their capability is limited in capturing nonlinear relationships and complex temporal variability. Advancements in machine learning, particularly Artificial Neural Networks (ANN) [4], [8], have demonstrated improved accuracy in solar radiation prediction compared to statistical methods. However, these approaches generally still treat each observation location as an independent entity [9], [10].

With the advancement of deep learning, models based on Long Short-Term Memory (LSTM) and Recurrent Neural Networks (RNN) have been widely used to model temporal dependencies in solar radiation data [11]. Several studies report that LSTM is capable of yielding better prediction performance, especially under clear weather conditions [12]. Nonetheless, this model still has limitations as it does not explicitly consider the spatial influence of surrounding observation locations, despite the fact that atmospheric phenomena affecting solar radiation are regional and interconnected [13].

Spatio-temporal approaches based on CNN-LSTM and ConvLSTM have been developed to address these limitations, particularly for grid-based or satellite image data [14], [15]. Although effective in certain contexts, these approaches are less flexible when applied to irregularly geographically distributed observation station networks, such as the BMKG AWS network [16]. Grid-based spatial representations also do not always reflect the actual geographical relationships between locations [17].

Representing data in the form of graphs offers a more flexible alternative for modeling the interconnections between observation locations. In this approach, each station is represented as a node, while spatial relationships between stations are modeled as edges based on geographical proximity or specific characteristics. Graph Neural Networks (GNN) were developed to process graph-based data and have shown promising performance in various environmental and renewable energy applications [18], [19]. Several studies report that GNN can improve the accuracy of solar energy and photovoltaic power predictions by leveraging spatial dependencies between locations [20], [21].

Nevertheless, the application of GNN for solar radiation estimation based on multi-location AWS data in tropical regions remains relatively limited in the literature. Furthermore, most previous studies have focused more on global or regional evaluations, without designating a single location as the main focus of analysis. Therefore, this research is directed towards addressing this gap by proposing a GNN-based spatio-temporal approach for solar radiation estimation, with a specific focus on Sawahan Subdistrict as the target location.

This study aims to evaluate the capability of Graph Neural Networks in modeling the spatial and temporal influences of solar radiation by utilizing multi-location data from the area around Sawahan. By designating Sawahan as the target node and other locations as supporting nodes, this research is expected to provide a practical contribution to location-based solar energy potential assessment and to support regional-level solar energy planning.

Based on the identified research gap, this study makes several scientific contributions. First, this research develops a spatio-temporal modeling framework that integrates Graph Convolutional Networks (GCN) and Long Short-Term Memory (LSTM) to estimate solar irradiance using multi-location Automatic Weather Station (AWS) data. Second, the proposed approach is specifically designed for an irregularly distributed observation network in a tropical region, where conventional grid-based spatial models are less effective. Third, this study adopts a target-node-oriented evaluation by focusing on Sawahan Subdistrict as the primary location of interest, while surrounding stations act as supporting nodes to capture spatial atmospheric interactions. These contributions demonstrate the effectiveness of graph-based spatial aggregation for localized solar

irradiance estimation and provide practical insights for regional solar energy assessment in data-scarce environments.

## 2. METHODS

This study focuses on Sawahan Subdistrict, Nganjuk Regency, East Java, as the primary target location for solar radiation estimation. Sawahan was selected due to its geographical characteristics situated in a hilly area with relatively high weather variability, thus demanding a modeling approach capable of capturing spatial and temporal interconnections simultaneously [22].

The data used originates from five Automatic Weather Stations (AWS) owned by the Indonesian Agency for Meteorology, Climatology, and Geophysics (BMKG), distributed across Nganjuk Regency and its surrounding areas. As presented in Table 1, the observational data includes parameters of global solar radiation with a 30-minute temporal resolution during the period of January–December 2024.

**Table 1.** Dataset from Automatic Weather Station (AWS)

Time	Kediri	Paron	Sawahan	Sebayi	Unida
	sr_avg	sr_avg	sr_avg	sr_avg	sr_avg
00:00	0	0	0	104,6	235
00:10	161,8	161,8	322	286,1	275
00:20	184,9	184,9	369	316,8	292
...	...	...	...	...	...
23:30	112,4	112,4	158	151	128
23:40	129,6	129,6	155	148	124
23:50	149,8	149,8	155	161	124

This resolution was selected to maintain data stability and to avoid information loss due to missing data or extreme noise at more granular intervals. Table 2 presents the location information of the observation stations used in this study.

**Table 2.** Location of Automatic Weather Stations Used in This Study

Station Code	Latitude (°)	Longitude (°)	Role in Graph
AWS-KDR	-78.167	120.167	Supporting Node
AWS-PRN	-74.419	113.879	Supporting Node
AWS-SWH	-77.412	117.605	Target Node (Sawahan)
AWS-SBY	-76.008	117.458	Supporting Node
AWS-UND	-78.860	114.940	Supporting Node

**2.1. Graph Construction**

To represent the spatial relationships between observation locations, the AWS data were modeled in the form of an undirected graph. Each station is represented as a node, while edges are formed based on the geographical proximity between stations. Edge weights were determined using a Euclidean distance function based on latitude and longitude coordinates. This approach enables a more realistic modeling of spatial relationships compared to conventional grid representations [23]. The Sawahan node is treated as the target node, while the other stations serve as supporting nodes that provide additional spatial information. The spatial graph representation used in this study is shown in Figure 1.

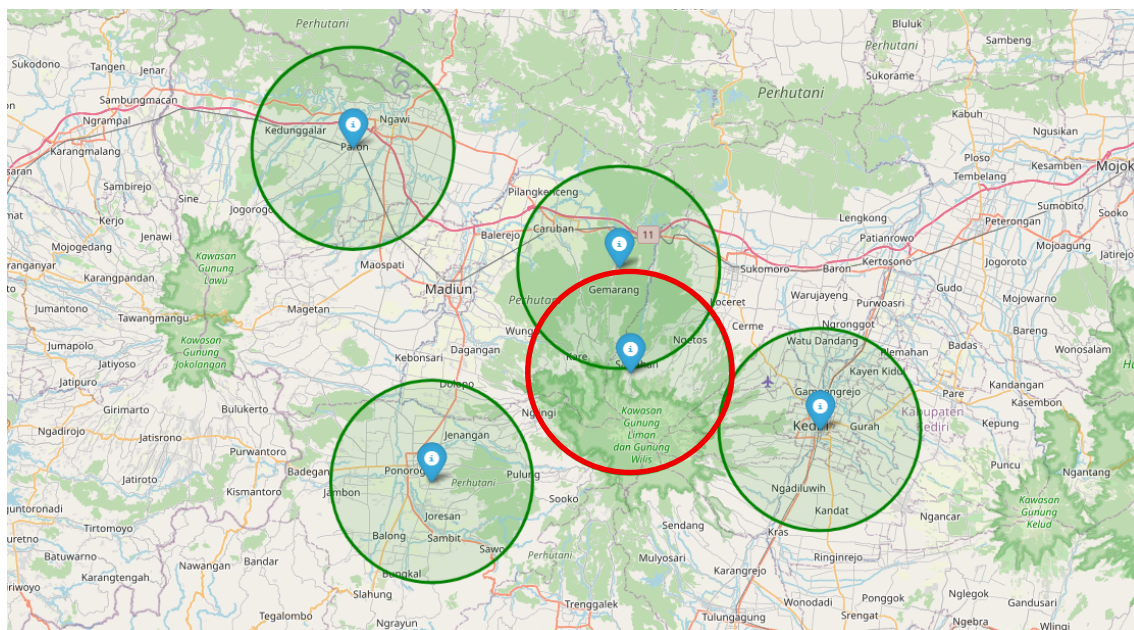


**Figure 1.** Spatial Graph Representation of AWS Network with Sawahan as Target Node

The station observation network is represented as an undirected graph,  $G = (\mathcal{V}, \mathcal{E}, \mathbf{A})$  where  $\mathcal{V}$  denotes the set of nodes representing the AWS stations,  $\mathcal{E}$  is the set of edges connecting the nodes, and  $\mathbf{A} \in \mathbf{R}^{N \times N}$  is the adjacency matrix [24]. The edge weight between nodes  $i$  and  $j$  is determined based on geographical distance using Euclidean distance as shown in Equation 1.

$$d_{ij} = \sqrt{(\text{lat}_i - \text{lat}_j)^2 + (\text{lon}_i - \text{lon}_j)^2} \quad (1)$$

where  $\text{lat}_i$  and  $\text{lon}_i$  denote the latitude and longitude coordinates of the- $i$  station, respectively. The weight value in the adjacency matrix is then defined as shown in Equation 2.

$$A_{ij} = \begin{cases} \exp(-d_{ij}), & i \neq j \\ 1, & i = j \end{cases} \quad (2)$$

This formulation aims to assign a higher weight to nodes that are geographically closer, while preserving the information of each node itself through the self-loop. This approach enables the graph to represent the actual spatial relationships between observation locations without relying on a rigid grid structure, making it more suitable for irregularly distributed AWS networks.

## 2.2. Spatio-Temporal Modeling Using GNN

To extract spatial features from the constructed graph, a Graph Convolutional Network (GCN) is employed [25]. The graph convolution operation at the- $l$  layer is defined shown in Equation 3.

$$h_i^{(l+1)} = \sigma \left( \sum_{j \in \mathcal{N}(i)} W^{(l)} h_j^{(l)} + b^{(l)} \right) \quad (3)$$

The adopted modeling approach integrates a Graph Convolutional Network (GCN) and Long Short-Term Memory (LSTM) to capture spatial and temporal dependencies simultaneously [26]. The GCN is used to extract spatial features among nodes in the

graph, while the LSTM models the temporal dependencies within the solar radiation data [21], [27].

At each timestep, the solar radiation features from all nodes are processed through the GCN layer to generate an aggregated spatial representation. This representation is then fed as input to the LSTM layer to learn short- and medium-term temporal patterns. The integration of these two components forms a spatio-temporal Graph Neural Network framework capable of representing solar radiation dynamics more comprehensively [28]. The proposed spatio-temporal modeling pipeline is illustrated in Figure 2.

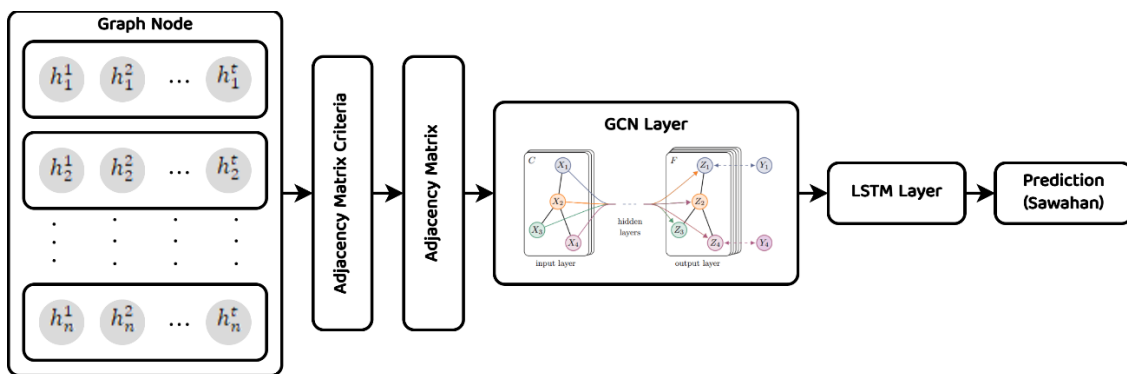


**Figure 2.** Architecture of the Proposed Spatio-Temporal GNN Model

The model was trained using historical data with a temporal split into training and test sets to preserve temporal consistency. The training process minimized the *Mean Squared Error* (MSE) loss function using the Adam optimizer. It should be noted that the LSTM component in this study is not treated as a standalone baseline model. Instead, LSTM is integrated as the temporal modeling module within the proposed spatio-temporal GCN-LSTM framework, following spatial feature aggregation by the GCN layer. Therefore, no separate single-station LSTM baseline experiment is conducted.

The model's performance was evaluated using several quantitative metrics: *Mean Absolute Error* (MAE), *Root Mean Squared Error* (RMSE), and the coefficient of determination ( $R^2$ ). Evaluation focused on the solar radiation estimation results for Sawahan, while the performance on other nodes served as supporting information for spatial analysis. The model's performance is defined shown in Equation 4 and 5.

$$MAE = \frac{1}{n} \sum_{i=1}^n |y_i - \hat{y}_i| \quad (4)$$

$$RMSE = \sqrt{\frac{1}{n} \sum_{i=1}^n (y_i - \hat{y}_i)^2} \quad (5)$$

The entire modeling and evaluation process was implemented using the Python programming language, supported by deep learning and graph processing libraries. The model implementation was designed to be replicable and adaptable for other regions with similar spatial characteristics.

The dataset was divided into training and testing subsets using a temporal split to preserve chronological consistency. Specifically, 80% of the earlier observations were used for model training, while the remaining 20% of the most recent data were reserved for testing. The model uses the hyperparameters summarized in Table 3.

**Table 3.** Hyperparameter Settings of the Proposed GCN–LSTM Model

Hyperparameter	Value
Graph convolution layers	1
GCN hidden units	64
LSTM hidden units	64
Sequence length (timesteps)	24
Learning rate	0.001
Optimizer	Adam
Loss function	Mean Squared Error (MSE)
Batch size	32
Number of epochs	100
Train–test split	80% (train) – 20% (test, temporal split)

### 3. RESULTS AND DISCUSSION

This section presents the experimental results obtained from the proposed spatio-temporal Graph Neural Network (GNN) model for solar irradiance estimation. The results

are reported in terms of quantitative evaluation metrics, prediction performance at the target location, and visual comparison between observed and predicted values.

### 3.1. Spatial Effect on Sawahan as Target Node

As the target node, Sawahan exhibited high sensitivity to information from its nearest supporting nodes. The distance-based spatial connections enabled the model to utilize data from stations with similar weather characteristics. Figure 3 illustrates the influence of spatial aggregation on the solar radiation estimation results for Sawahan. This approach proved effective in reducing extreme prediction fluctuations that commonly arise in single-node models.

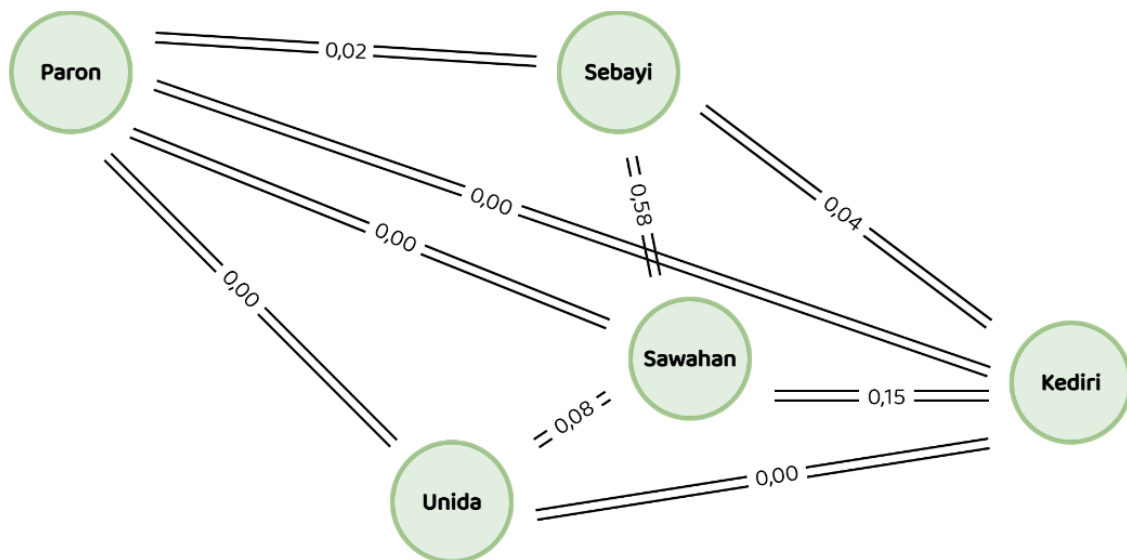


**Figure 3.** Effect of Spatial Aggregation on Solar Irradiance Estimation in Sawahan

### 3.2. Model Training Performance

During the training process, the model exhibited a stable convergence pattern. The loss value decreased consistently over successive epochs, indicating effective learning behavior. No significant divergence or instability was observed throughout the training phase. The performance training is presented in Figure 4.

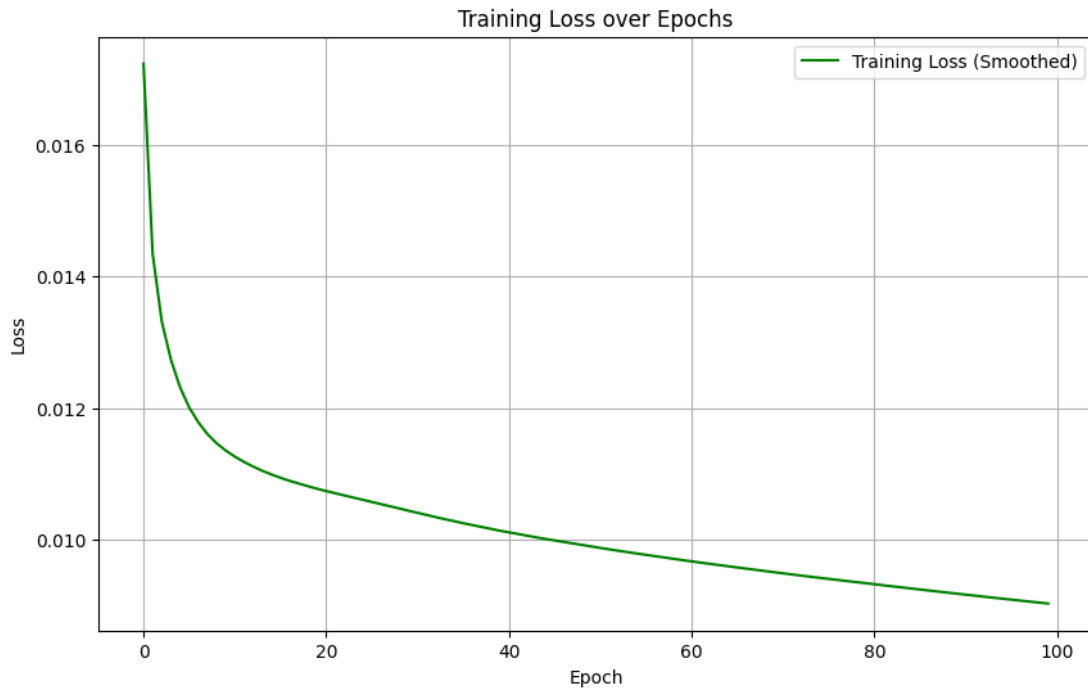


**Figure 4.** Training Loss Curve

### 3.3. Quantitative Evaluation Results

The predictive performance of the proposed model was evaluated using standard regression metrics, including Mean Absolute Error (MAE), Root Mean Squared Error (RMSE), and the coefficient of determination ( $R^2$ ). The evaluation was conducted on the testing dataset for the target location [29]. The obtained performance metrics are summarized in Table 4.

**Table 4.** Prediction Performance Metrics at the Target Location (Sawahan)

Metric	Value
MAE	102.64 Watt/m <sup>2</sup>
RMSE	166.76 Watt/m <sup>2</sup>
$R^2$	0.6446

### 3.4. Prediction Results at the Target Location

Figure 5 illustrates the comparison between observed and predicted solar irradiance values at the target location over the testing period. The predicted values follow the

general temporal pattern of the observed data, including daily irradiance peaks and troughs. Presents a time-series visualization comparing observed and predicted solar irradiance values over selected periods. The visualization highlights the model's ability to track short-term temporal variations across multiple time.

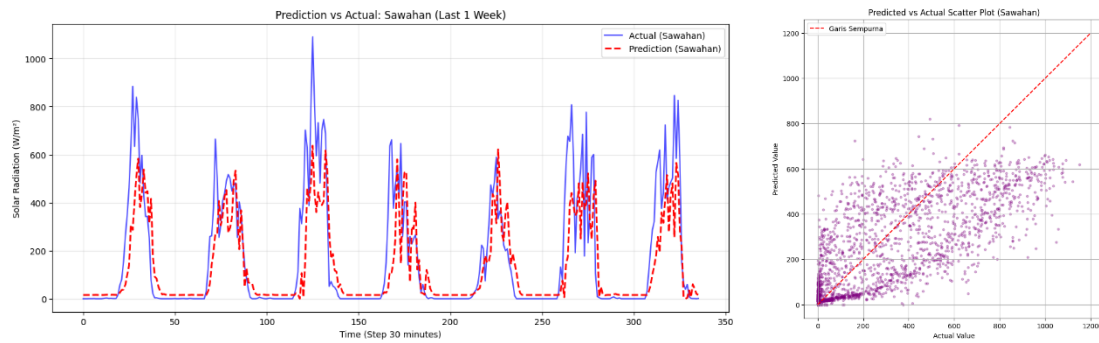


**Figure 5.** Observed vs. Predicted Solar Irradiance at Sawahan

### 3.5. Error Distribution Analysis

To further examine prediction behavior, the distribution of prediction errors was analyzed. Figure 6 presents the histogram of residual errors between observed and predicted irradiance values.

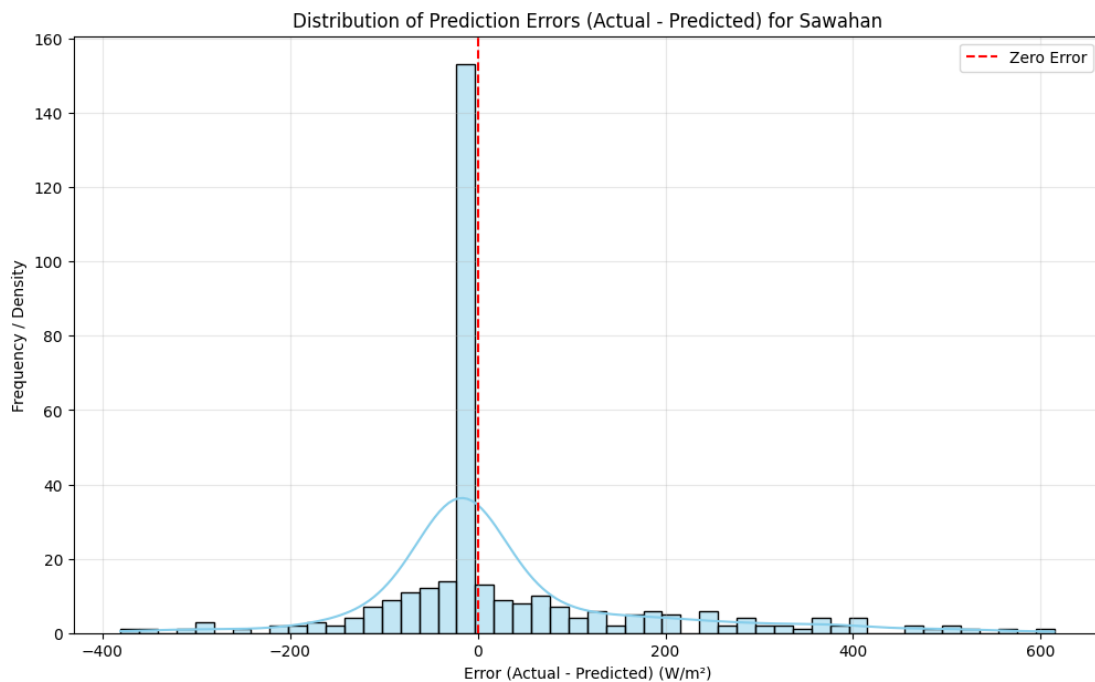


**Figure 6.** Error Distribution of Solar Irradiance Predictions

The experimental results demonstrate that the proposed GNN-based model produces consistent solar irradiance predictions for the target location. The quantitative metrics and visual analyses provide a comprehensive overview of model performance under the evaluated conditions.

### 3.6. Discussion

This study evaluated a spatio-temporal Graph Neural Network (GCN-LSTM) for estimating solar irradiance at Sawahan Subdistrict using multi-location BMKG AWS observations. Overall, the experimental results show that the proposed framework can learn meaningful spatial-temporal relationships and provide stable predictions for a target-node-oriented setting, which is particularly relevant for tropical regions where irradiance variability is strongly driven by fast-changing cloud dynamics and local terrain effects.

Quantitatively, the model achieved an MAE of 102.64 W/m<sup>2</sup>, an RMSE of 166.76 W/m<sup>2</sup>, and an R<sup>2</sup> of 0.6446 at the target node (Table 4). These values indicate moderate-to-good explanatory capability for a single-variable irradiance estimation task in a complex, heterogeneous environment such as Sawahan. The R<sup>2</sup> value suggests the model explains roughly 64% of the observed variance, meaning the remaining variability is likely associated with factors not explicitly represented in the input (e.g., cloud optical thickness, humidity, rainfall events, aerosol loading, and micro-topographic shading). Importantly, the gap between RMSE and MAE also implies the presence of occasional larger errors, which is consistent with irradiance behavior during rapid transitions between clear-sky and overcast conditions. In practice, such “spikes” are common in tropical convective regimes and can dominate RMSE even when day-to-day patterns are captured well.

A key implication of the results is the value of spatial aggregation for improving the reliability of irradiance estimation at the target station. Unlike single-location time-series models that only learn temporal autocorrelation from one sensor, the proposed approach first extracts spatial features through the GCN and then models temporal dependencies through the LSTM. This ordering is important: spatial aggregation provides the LSTM with a more informative representation of regional atmospheric state, rather than forcing the temporal model to infer regional changes from local history alone. The qualitative outcome of this design is reflected in the spatial effect observed for Sawahan (Figure 3),

where graph-based neighborhood information helps reduce extreme fluctuations that are often driven by localized noise or short-lived measurement variability. The distance-weighted adjacency matrix (Equations 1–2) further supports this by giving greater influence to geographically closer stations, which are more likely to experience correlated cloud evolution and synoptic patterns.

From a learning behavior perspective, the training curve (Figure 4) shows stable convergence without noticeable divergence, suggesting the model capacity and optimization settings were appropriate for the dataset scale and the selected hyperparameters (Table 3). The relatively simple architecture—one GCN layer followed by an LSTM—appears sufficient to capture the dominant spatial interactions among the five AWS nodes while maintaining training stability. This is a practical advantage in regional operational contexts, where overly complex models can be harder to tune and may overfit when station networks are small.

The temporal prediction plots at Sawahan (Figure 5) indicate that the model tracks the diurnal irradiance cycle effectively, reproducing the general rise in the morning, midday peaks, and afternoon decline. This behavior is consistent with the LSTM's strength in learning short-to-medium temporal dependencies. However, the model's deviations increase during periods of unstable atmospheric conditions, especially when cloud cover changes abruptly. This is expected: irradiance can drop sharply within minutes under convective cloud development, and such transitions are difficult to predict accurately using irradiance-only signals. In these situations, the graph component helps by leveraging neighboring stations that may observe the same cloud system earlier or more clearly, but it cannot fully resolve events that are highly localized or occur between stations.

The residual error distribution (Figure 6) provides additional insight into model behavior. A well-performing regression model typically produces residuals centered near zero with limited skewness, while heavy tails indicate occasional large deviations. In this study, the combination of an RMSE notably larger than MAE suggests that while the model performs consistently most of the time, rare high-magnitude errors still occur—likely tied to sudden cloud passages or localized shading effects in hilly terrain. This finding supports the interpretation that the proposed framework is robust for typical conditions but

remains challenged by rapidly evolving micro-scale phenomena that are not fully observable through a sparse station network.

Practically, the proposed GCN–LSTM framework is promising for solar energy assessment and planning in regions with limited observation infrastructure. Because the method relies on existing AWS networks and models spatial correlation directly on irregular station layouts, it is well suited for environments where dense sensor deployment or satellite-image-based approaches are not feasible. For planning-level applications—such as preliminary PV potential mapping, site screening, or regional resource assessment—the achieved error range can be considered operationally useful, especially when combined with aggregation over longer timescales (e.g., hourly/daily energy estimates) where random short-term errors tend to cancel out.

Nevertheless, several limitations should be noted. First, the spatial graph is constructed from only five stations, which restricts the richness of spatial patterns the model can learn and may limit generalization under atypical weather regimes. Second, the model uses solar irradiance as the primary variable, meaning it must infer atmospheric state changes indirectly. Incorporating additional meteorological predictors (e.g., temperature, relative humidity, wind speed, rainfall, pressure, or cloud-related proxies) would likely improve performance during rapidly changing conditions. Third, while this work intentionally focuses on evaluating the contribution of graph-based spatial aggregation, the absence of explicit baseline experiments (e.g., persistence, single-station LSTM, ARIMA, or tree-based regressors) limits the ability to quantify the exact gain attributable to the graph component.

Future work can build on these results in several directions: (1) expanding the AWS network to improve spatial coverage and reduce uncertainty in localized events, (2) integrating multi-variable meteorological features and deterministic solar geometry inputs (e.g., solar zenith angle, day-of-year seasonality), (3) exploring more advanced spatio-temporal GNN architectures (e.g., attention-based GNNs, diffusion-based models, or dynamic graphs that adapt connectivity over time), and (4) adding uncertainty estimation (e.g., quantile loss or ensemble modeling) to better characterize reliability during extreme cloud transitions.

The results confirm that spatial dependencies are critical for localized irradiance estimation in heterogeneous tropical terrain. By combining distance-aware graph aggregation with temporal sequence learning, the proposed GCN-LSTM model provides a practical and extensible foundation for target-location solar irradiance estimation using irregular AWS station networks.

#### 4. CONCLUSION

This study has presented a spatio-temporal modeling approach for solar irradiance estimation using Graph Neural Networks (GNN) based on multi-location Automatic Weather Station (AWS) data. The proposed framework integrates spatial relationships among observation sites through graph-based aggregation and captures temporal dependencies using Long Short-Term Memory (LSTM). The model was evaluated using real-world data from Nganjuk Regency, with Sawahan Subdistrict designated as the target location. The experimental results demonstrate that the proposed GNN-based model is capable of producing reliable solar irradiance estimates, as reflected by the achieved MAE, RMSE, and  $R^2$  values. By incorporating spatial information from surrounding stations, the model effectively captures regional atmospheric interactions that are not represented in single-station approaches.

The findings of this study highlight the importance of spatial dependency modeling for localized solar irradiance estimation, particularly in tropical regions characterized by high weather variability and irregular observation networks. From a practical perspective, the proposed framework can support regional solar energy potential assessment by utilizing existing meteorological infrastructure. Despite these contributions, several limitations should be acknowledged. The current implementation is based on a limited number of observation stations and focuses solely on solar irradiance parameters. Future research may extend this work by integrating additional meteorological variables, expanding the spatial network, and exploring more advanced GNN architectures to further improve estimation accuracy and generalization capability.

## FUNDING

The authors declare that no external funding was received for this research. All activities related to this study were fully supported and financed by the authors themselves.

## AUTHOR CONTRIBUTIONS STATEMENT

First Author (Agung Wilis Nurcahyo): Conceptualization, methodology, software, formal analysis, investigation, data curation, writing–original draft, writing–review & editing, visualization, and project administration. Second Author (Bambang Purnomosidi Dwi Putranto): Methodology, validation, resources, writing–review & editing, and supervision.

## CONFLICT OF INTEREST STATEMENT

The authors declare that there are no conflicts of interest in the writing of this article.

## DATA AVAILABILITY

The dataset used in this research is not open access.

## REFERENCES

- [1] H. Wu, I. Budi, S. West, and M. Almashor, "Floating utility-scale photovoltaic site selection in Indonesia: a Multi-Criteria Decision Analysis approach," *Int. J. Sustain. Energy*, vol. 45, no. 1, Dec. 2026, doi: 10.1080/14786451.2025.2607911.
- [2] C. Y. Wang and P. C. Hsu, "Integrated geospatial evaluation of wind and photovoltaic resources based on multi-satellite and ground-validated datasets," *Int. J. Sustain. Energy*, vol. 44, no. 1, Dec. 2025, doi: 10.1080/14786451.2025.2565330.
- [3] T. Sucita, D. L. Hakim, R. H. Hidayatulloh, and D. Fahrizal, "Solar irradiation intensity forecasting for solar panel power output analyze," *Indones. J. Electr. Eng. Comput. Sci.*, vol. 36, no. 1, pp. 74–85, Oct. 2024, doi: 10.11591/ijeecs.v36.i1.pp74-85.

- [4] R. Rimbawati, H. Ambarita, T. Burhanuddin Sitorus, and M. Irwanto, "Artificial Neural Network (ANN) Backpropagation for Forecasting 100% Renewable Energy in North Sumatera," *Environ. Res. Eng. Manag.*, vol. 81, no. 1, pp. 87–101, Mar. 2025, doi: 10.5755/j01.erem.81.1.37767.
- [5] M. Baloch, M. S. Honnurvali, A. Kabbani, T. Ahmed, S. T. Chauhdary, and M. S. Saeed, "Solar Energy Forecasting Framework Using Prophet Based Machine Learning Model: An Opportunity to Explore Solar Energy Potential in Muscat Oman," *Energies*, vol. 18, no. 1, p. 205, Jan. 2025, doi: 10.3390/en18010205.
- [6] M. L. Hossain, S. M. N. Shams, and S. M. Ullah, "Time-series and deep learning approaches for renewable energy forecasting in Dhaka: a comparative study of ARIMA, SARIMA, and LSTM models," *Discov. Sustain.*, vol. 6, no. 1, p. 775, Aug. 2025, doi: 10.1007/s43621-025-01733-5.
- [7] G. Wibowo, B. P. D P, and W. Andriyani, "Multiple Linier Regression Analysis Effects of Education Media on Student Experience and Satisfaction," *Sinkron*, vol. 9, no. 4, pp. 2061–2069, Oct. 2025, doi: 10.33395/sinkron.v9i4.15293.
- [8] S. Knežević and M. Žarković, "Artificial intelligence modeling for power system planning," *Electr. Eng.*, vol. 107, no. 3, pp. 2535–2549, Aug. 2025, doi: 10.1007/s00202-024-02652-w.
- [9] Harmini and T. Nurhayati, "Prediksi Power Solar Energy Melalui Solar Photovoltaic (SPV) menggunakan Artificial Neural Network – Radial Basic Function (ANN-RBF)," *Simetris J. Tek. Mesin, Elektro dan Ilmu Komput.*, vol. 3, no. 5, p. 6, Nov. 2021, doi: 10.24176/simet.v12i2.6897.
- [10] G. S, M. S, and S. G, "Solar Power Forecasting Using Artificial Neural Networks," *ESP J. Eng. Technol. Adv.*, vol. 3, no. 3, pp. 119–124, 2023.
- [11] A. Mahalingam, S. Thatte, Y. Narkhede, Y. Brid, and D. Mane, "A survey of photovoltaic power forecasting approaches in solar energy landscape," in *Computational Methods in Science and Technology - Proceedings of the 4th International Conference on Computational Methods in Science and Technology, ICCMST 2024*, vol. 2, London: CRC Press, 2025, pp. 87–101. doi: 10.1201/9781003561651-13.
- [12] M. V. Nugroho, F. Mardiansah, T. O. Pratama, Z. A. Fikriyadi, D. V. Dianti, and A. Prastawa, "A Comparative Study of the Effect of Weather Conditions on Solar Irradiance Forecasting Using Various Methods in Yogyakarta, Indonesia," *J. Phys. Conf. Ser.*, vol. 2828, no. 1, p. 012028, Oct. 2024, doi: 10.1088/1742-6596/2828/1/012028.

- [13] M. AlKandari and I. Ahmad, "Solar power generation forecasting using ensemble approach based on deep learning and statistical methods," *Appl. Comput. Informatics*, vol. 20, no. 3–4, pp. 231–250, Jun. 2024, doi: 10.1016/j.aci.2019.11.002.
- [14] T. Bashir, H. Wang, M. Tahir, and Y. Zhang, "Wind and solar power forecasting based on hybrid CNN-ABiLSTM, CNN-transformer-MLP models," *Renew. Energy*, vol. 239, p. 122055, Feb. 2025, doi: 10.1016/j.renene.2024.122055.
- [15] L. Liao, M. Tao, A. Dong, R. Xie, and Y. Zhang, "Graph-Convolutional-Network-Enabled Task Offloading for Industrial Image Recognition in Digital Twin Edge Networks," *IEEE Internet Things J.*, vol. 12, no. 15, pp. 29176–29188, Aug. 2025, doi: 10.1109/JIOT.2025.3543521.
- [16] A. Gufron *et al.*, "A preliminary LSTM-IDW model for spatiotemporal hourly solar radiation estimation in tropical regions," *Renew. Sustain. Energy Transit.*, vol. 7, p. 100105, Jun. 2025, doi: 10.1016/j.rset.2025.100105.
- [17] A. Alcañiz, D. Grzebyk, H. Ziar, and O. Isabella, "Trends and gaps in photovoltaic power forecasting with machine learning," *Energy Reports*, vol. 9, pp. 447–471, Dec. 2023, doi: 10.1016/j.egy.2022.11.208.
- [18] Z. Ye, Y. J. Kumar, G. O. Sing, F. Song, and J. Wang, "A Comprehensive Survey of Graph Neural Networks for Knowledge Graphs," *IEEE Access*, vol. 10, pp. 75729–75741, 2022, doi: 10.1109/ACCESS.2022.3191784.
- [19] P. Cui, L. Wu, J. Pei, L. Zhao, and X. Wang, *Graph Representation Learning*. in Synthesis Lectures on Artificial Intelligence and Machine Learning. Cham: Springer International Publishing, 2022. doi: 10.1007/978-981-16-6054-2\_2.
- [20] N. Zhu, Y. Wang, K. Yuan, J. Yan, Y. Li, and K. Zhang, "GGNet: A novel graph structure for power forecasting in renewable power plants considering temporal lead-lag correlations," *Appl. Energy*, vol. 364, p. 123194, Jun. 2024, doi: 10.1016/j.apenergy.2024.123194.
- [21] S. Xia *et al.*, "GCN-LSTM Based Transient Angle Stability Assessment Method for Future Power Systems Considering Spatial-temporal Disturbance Response Characteristics," *Prot. Control Mod. Power Syst.*, vol. 9, no. 6, pp. 108–121, Nov. 2024, doi: 10.23919/PCMP.2023.000116.
- [22] T. A. Laksono, W. Andriyani, F. G. Putra, I. F. Ruas da silva, and W. Widayani, "Digital Activity Location Clustering Based on Twitter Geospatial Data for Spatiotemporal Business Intelligence," *J. Intell. Softw. Syst.*, vol. 4, no. 1, p. 22, Jul. 2025, doi: 10.26798/jiss.v4i1.2005.

- [23] A. Armghan, J. Logeshwaran, S. Raja, K. Aliqab, M. Alsharari, and S. K. Patel, "Performance optimization of energy-efficient solar absorbers for thermal energy harvesting in modern industrial environments using a solar deep learning model," *Heliyon*, vol. 10, no. 4, p. e26371, Feb. 2024, doi: 10.1016/j.heliyon.2024.e26371.
- [24] C. C. Aggarwal, *Neural Networks and Deep Learning: A Textbook*. Cham: Springer International Publishing, 2023. doi: 10.1007/978-3-031-29642-0.
- [25] C. Gao, J. Zhu, F. Zhang, Z. Wang, and X. Li, "A Novel Representation Learning for Dynamic Graphs Based on Graph Convolutional Networks," *IEEE Trans. Cybern.*, vol. 53, no. 6, pp. 3599–3612, Jun. 2023, doi: 10.1109/TCYB.2022.3159661.
- [26] S. Asiedu, A. Suvedi, Z. Wang, H. Reabdarkolae, and T. Hansen, "Spatiotemporal Downscaling Model for Solar Irradiance Forecast Using Nearest-Neighbor Random Forest and Gaussian Process," *Energies*, vol. 18, no. 10, p. 2447, May 2025, doi: 10.3390/en18102447.
- [27] B. A. Wisesa, W. Andriyani, and B. D. P. Purnomosidi, "Usage of LSTM Method on Hand Gesture Recognition for Easy Learning of Sign Language Based on Desktop Via Webcam," in *2022 5th International Seminar on Research of Information Technology and Intelligent Systems, ISRITI 2022*, IEEE, Dec. 2022, pp. 148–153. doi: 10.1109/ISRITI56927.2022.10053076.
- [28] A. Deng and B. Hooi, "Graph Neural Network-Based Anomaly Detection in Multivariate Time Series," *35th AAAI Conf. Artif. Intell. AAAI 2021*, vol. 5A, no. 5, pp. 4027–4035, May 2021, doi: 10.1609/aaai.v35i5.16523.
- [29] S. Pewekar, M. Tirkey, A. Mallik, R. Shaikh, and S. A. Wagle, "Diabetes Prediction Using Machine Learning," *Lect. Notes Electr. Eng.*, vol. 1196 LNEE, no. 3, pp. 67–76, Oct. 2024, doi: 10.1007/978-981-97-7862-1\_5.